JOURNAL OF MATERIALS SCIENCE 22 (1987) 3931–3938

The magnetic properties of the glassy ferromagnets $Fe_{81.5}B_{14.5}Si_4$ and $Fe_{40}Ni_{40}B_{20}$

E. E. SHAISHA, A. A. BAHGAT, M. H. EL-KOTTAMY, N. A. EISSA
Department of Physics, Faculty of Science, Al-Azhar University, Nasr Ciry, Cairo, Egypt

The glassy ferromagnets $Fe_{81.5}B_{14.5}Si_4$ and $Fe_{40}Ni_{40}B_{20}$ have been studied by Mössbauer spectroscopy from 77.5 up to 650 and 680 K, respectively. In the glassy state, the average magnetic hyperfine field decreases with increasing temperature due to a distribution of exchange interactions. At low temperature $H(T)/H(0)$ has a temperature dependence $(1 - BT^{3/2} - CT^{5/2})$ where B and C are constants, indicative of spin-wave excitations in glassy ferromagnets. The value of $B_{3/2} = 0.40 \pm 0.05$ is almost four times larger than those of crystalline iron and nickel. On the other hand, fluctuations of the exchange interaction constant are found to decrease with increasing temperature. The Curie temperatures $T_c = 608$ K for the glassy $Fe_{81.5}B_{14.5}Si_4$ and $T_c = 593$ K for the glassy $Fe_{40}Ni_{40}B_{20}$ are found to be well defined. At T close to T_c, $H(T)$ behaves as a power law with critical exponent $\beta = 0.3$. The crystallization T_{cr} for a glassy $Fe_{81.5}B_{14.5}Si_4$ was found to be 645 K. The crystalline material obtained contains three different phases, namely α-Fe, Fe_2B and Fe–8% Si.

1. Introduction

The magnetic metallic glasses produced by rapid quenching of a melt of iron-based transition-metal–metalloid systems have been of scientific technological interest in the recent past (see e.g. [1, 2]). Although these glasses lack long-range crystalline order they show ferromagnetic order [3]. Due to the random or disordered atomic arrangement in magnetic-metallic glasses their characteristic magnetic parameters, like exchange interactions, magnetic moments, hyperfine fields, etc., have a distribution of value instead of unique values. Also, since the glassy state represents a metastable state they tend to show structural relaxation with time which gets accelerated at higher temperatures. At high enough temperatures they crystallize irreversibly to a more stable state. Crystallization usually destroys most of their useful magnetic and mechanical properties.

The most studied metallic glass system is Fe_xB_{1-x} $(0.72 \leqq x \leqq 0.86)$ which may even be called the basic magnetic metallic glass system [4–6]. In a binary system, it is easier to interpret experimental results theoretically. However, this has not satisfied the practical application requirements. A number of studies have been reported on Fe–B–Si metallic glasses, elucidating their electrical and magnetic properties and thermal stability [7–11].

In the present contribution, a detailed study of the glassy ferromagnets $Fe_{81.5}B_{14.5}Si_4$ and $Fe_{40}Ni_{40}B_{20}$ has been made by Mössbauer spectroscopy from 77.5 K up to 680 K.

2. Experimental technique

Amorphous ribbons of $Fe_{40}Ni_{40}B_{20}$ and $Fe_{81.5}B_{14.5}Si_4$ were supplied by Vitrovac (Hanau, West Germany) as-quenched, i.e. without any special optimization of magnetic or mechanical properties. The sample of $Fe_{40}Ni_{40}B_{20}$ had width 4 mm and thickness 40 μm while that of $Fe_{81.5}B_{14.5}Si_4$ had width 10 mm and thickness 30 μm. The Mössbauer measurements were performed using a constant-acceleration driving system. The source was ^{57}Co in a rhodium matrix. A ribbon about 10 cm long was cut into several pieces and these were placed in contact parallel to each other, the area covered being 2.5 cm^2. This arrangement of the pieces was placed between two rings of copper for measurements at room temperature. The measurements above room temperature were carried out in a vacuum oven with a temperature stability of ± 0.3 K. The liquid-nitrogen temperature (77 K) measurements were obtained by means of a suitable cryostat where the sample pieces were placed between two copper rings. The velocity calibration was performed using the standard spectrum of metallic iron with an inner line width of 0.25 mm sec^{-1}.

The magnetic ordering temperature (T_c) of the amorphous $Fe_{81.5}B_{14.5}Si_4$ was determined by the thermal scanning method. In this method, the count rate of the centroid of the spectrum is recorded as a function of temperature, with the transducer of the Mössbauer apparatus set at zero velocity. The counts in 400 sec were recorded while the temperature was raised from 300 to 650 K in steps of 2 K.

Computer fitting to the experimental results was performed assuming a Lorentzian shape. This shape fits the data points very well.

3. Results and discussion

Transmission Mössbauer spectra of the amorphous alloys $Fe_{81.5}B_{14.5}Si_4$ and $Fe_{40}Ni_{40}B_{20}$ at different temperatures are shown in Figs 1 and 2, respectively. The spectra show well-defined broadened lines. These line

0022–2461/87 $03.00 + .12

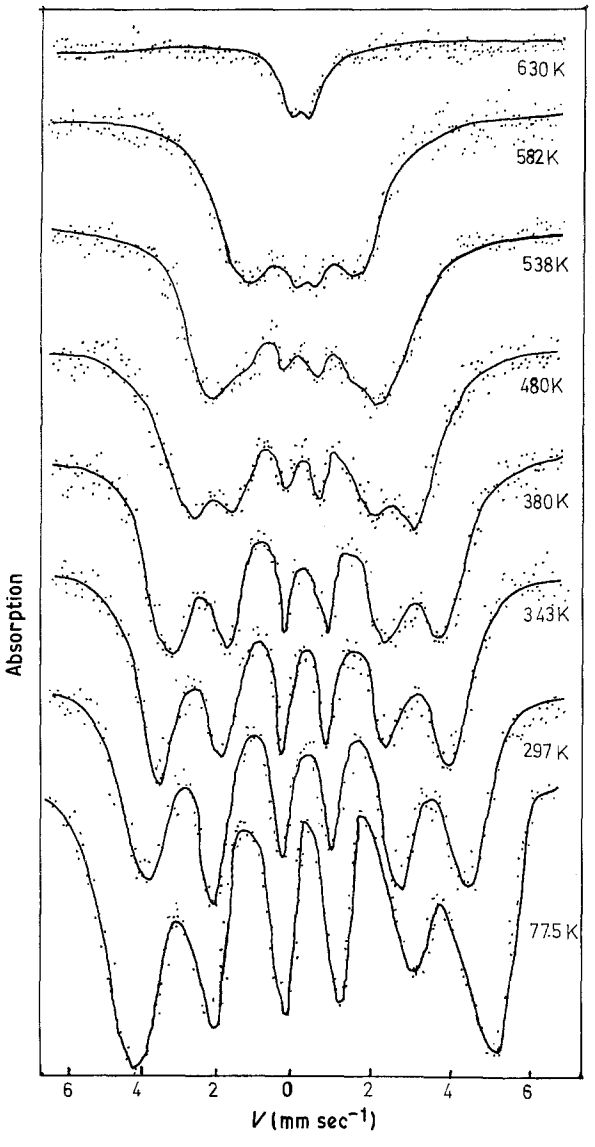

Figure 1 Mössbauer spectra of amorphous $Fe_{81.5}B_{14.5}Si_4$ at different temperatures.

widths are calculated for the alloy $Fe_{81.5}B_{14.5}Si_4$ to be $\Gamma_1 = 1.4$, $\Gamma_2 = 0.84$, $\Gamma_3 = 0.68$, $\Gamma_4 = 0.63$, $\Gamma_5 = 1.05$ and $\Gamma_6 = 1.37\,\text{mm sec}^{-1}$. Such spectral broadening is commonly observed in amorphous solids, and indicates that they do not represent a unique hyperfine magnetic field. This is expected from the non-crystalline nature of the samples in which there are many non-equivalent iron sites. The variations of Mössbauer parameters with temperature are summarized in Tables I and II, where the spectrum shift values are calculated with respect to iron metal.

It is more convenient to discuss the results obtained under the following subheadings.

3.1. Isomer shift, I.S.

The isomer shift has a temperature-dependent contribution which is caused by the motions of the emitting and absorbing nuclei. This kind of temperature dependence is known to be the result of the second-order Doppler shift. The temperature dependence can be approximated in many cases by assuming harmonic interatomic forces in the lattice. The two most widely used models to describe this dependence are the Einstein and Debye models, where the lattice is

TABLE I Mössbauer parameters obtained for the amorphous alloy $Fe_{81.5}B_{14.5}Si_4$

T (K)	I.S. (mm sec^{-1})	E_q (mm sec^{-1})	H_{eff} (T)	T/T_c
77.5	0.262	Zero	28.6	0.127
297	0.17	Zero	25.5	0.488
342.5	0.131	Zero	23.2	0.563
380	0.105	Zero	21.6	0.625
481	Zero	Zero	17.9	0.791
538.5	−0.078	Zero	13.3	0.88
582	−0.105	Zero	10.1	0.957
630	−0.157	0.42	–	–

characterized by the two temperatures θ_E and θ_D, respectively.

For a crystalline material, in which harmonic forces are assumed, the temperature dependence of the isomer shift becomes

$$\frac{d[\text{I.S.}(T)]}{dT} = -\frac{3kE_\gamma}{2Mc^2} \quad (1)$$

where c is the velocity of light, M is the atomic mass of the Mössbauer nucleus, k is the Boltzmann constant and E_γ is the gamma-ray energy which in this case is 14.4 keV. The slope given by the above equation comes out to be $-7.31 \times 10^{-4}\,\text{mm sec}^{-1}\,\text{K}^{-1}$ for ^{57}Fe atoms.

Figs 3a and b show the temperature dependence of the isomer shift for the two amorphous alloys studied; a linear variation can be seen above 200 K. The solid lines are a least-squares fit to the experimental data for $T \geqslant 300$ K using the slope given above.

The temperature dependence of $\ln A$, where A is the total area of the spectrum for the amorphous alloy $Fe_{81.5}B_{14.5}Si_4$, is shown in Fig. 4. The solid line is a good fit to the data points, with an effective $\theta_E = 168$ K and $\theta_D = 291$ K. These values satisfy the predicted ratio of $\theta_D/\theta_E = 3^{1/2}$, as given previously [12].

The good agreement between the experimental data and the calculated curves indicates that the dynamic model of atomic motion in these amorphous alloys is to a good approximation described by normal harmonic lattice vibration. The dotted curves in Figs 3a and b at low temperature are the extrapolations applying the harmonic approximation, which gives the expected value of isomer shift of 0.27 mm sec^{-1} for both the $Fe_{81.5}B_{14.5}Si_4$ and $Fe_{40}Ni_{40}B_{20}$ amorphous alloys.

The explanation of the harmonic behaviour could be accounted for here. For amorphous materials

TABLE II Mössbauer parameters obtained for the amorphous alloy $Fe_{40}Ni_{40}B_{20}$

T (K)	I.S. (mm sec^{-1})	E_q (mm sec^{-1})	H_{eff} (T)	T/T_c
77.5	0.26	Zero	26.1	0.135
297	0.168	Zero	22.6	0.52
373	0.105	Zero	20.97	0.65
473	Zero	Zero	17.4	0.825
593	0.118	0.5	–	–
608	0.15	0.48	–	–
663	0.21	0.5	–	–

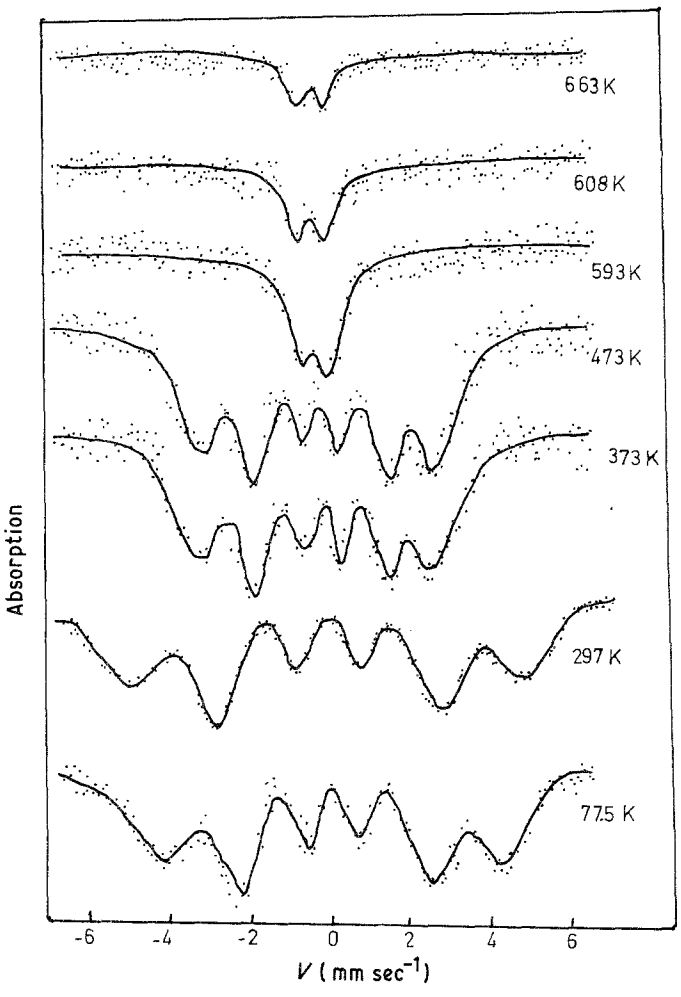

Figure 2 Mössbauer spectra of amorphous $Fe_{40}Ni_{40}B_{20}$ at different temperatures.

Cochrane and Strom-Oslen [13] propose that many atoms find themselves in atomic wells which are corrugated on a scale of a fraction of the average atomic spacing. For such atoms the atomic forces are not expected to be to a good approximation harmonic, at least not at low temperatures. However, Figs 3 and 4 show no difference between the experimental and calculated data. This result indicates either that the atomic forces are indeed harmonic or that the distortions leading to anharmonicity are not important for the thermal behaviour of these amorphous alloys.

3.2. Quadrupole interaction, ΔE_q

Screening by the conduction electrons reduces the quadrupole splitting in crystalline metals; in amorphous metals and alloys this effect can be expected to be important as well. Above the Curie temperature T_c, the quadrupole shift is given by

$$\varepsilon = \tfrac{1}{2}e^2QV_{zz}(1 + \tfrac{1}{3}\eta)^{1/2} \qquad (2)$$

where V_{zz} is the electric field gradient along the quantization axis, e is the electronic charge, Q is the quadrupole moment of the nucleus and η is the asymmetry parameter. Above T_c, the glassy samples are paramagnetic. On the other hand, below T_c, ε has been calculated from the positions of Mössbauer absorption lines from the expression

$$\varepsilon = \tfrac{1}{2}(V_6 - V_5 + V_1 - V_2) \qquad (3)$$

where V_i represents the position of the ith absorption line in mm sec^{-1}. Our results for the temperature dependence of the quadrupole shift ε show that, within

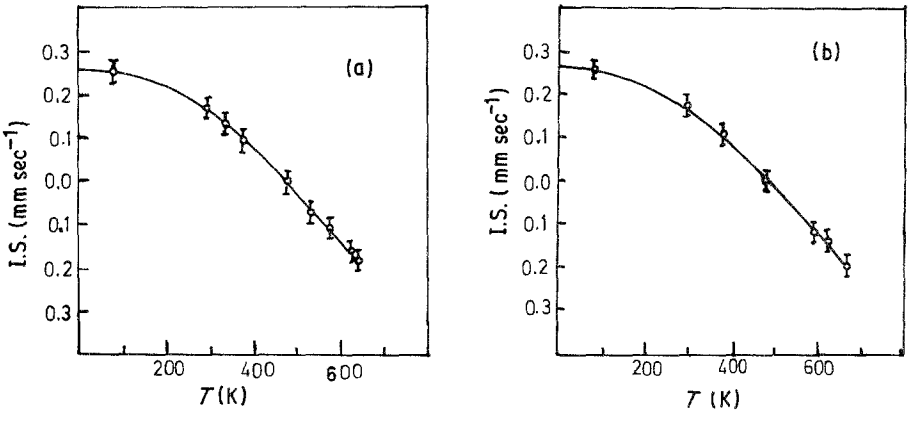

Figure 3 Isomer shift against temperature for (a) amorphous $Fe_{81.5}B_{14.5}Si_4$, (b) $Fe_{40}Ni_{40}B_{20}$.

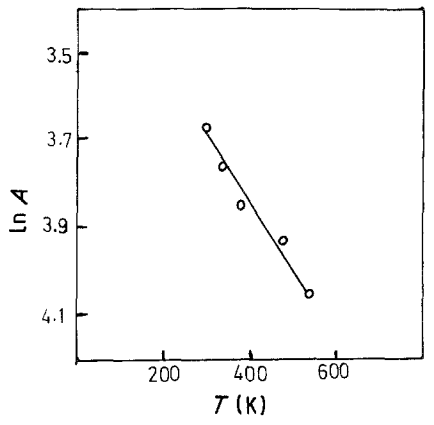

Figure 4 Change of $\ln A$ as a function of temperature for amorphous $Fe_{81.5}B_{14.5}Si_4$.

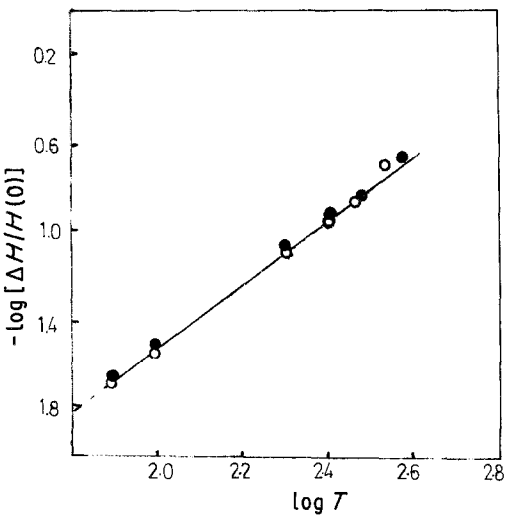

Figure 5 Changes of $[-\log(\Delta H/H(0))]$ against $\log T$ for amorphous (○) $Fe_{81.5}B_{14.5}Si_4$, (●) $Fe_{40}Ni_{40}B_{20}$.

experimental errors, all ε values are zero below T_c. This, in turn, means that the average value of the quadrupole splitting over all directions is zero. In other words, the magnetic hyperfine field is randomly oriented with respect to the principal axes of the electric field gradient.

3.3. Magnetic hyperfine field (MHF)

Because of the disordered structure in an amorphous solid, iron-site symmetry is generally non-cubic. At $T < T_c$ one expects a combination of magnetic and quadrupole interaction due to the non-zero electric field gradient (EFG) in all glassy solids. At a given iron site, i, the excited nuclear state of spin 3/2 due to combined magnetic and quadrupole interactions of a hyperfine field H and principal EFG eq_i, has energy levels of approximately

$$E = -g\mu_N Hm + (-1)^{|m|+1/2}\frac{eqQ}{4} \times \left(1 + \frac{\eta^2}{3}\right)^{1/2} \frac{3\cos^2\theta - 1}{2} \quad (4)$$

where m is the magnetic quantum number and θ is the angle between the direction of the principal EFG and that of the magnetic moment and where $g\mu_N$ is the nuclear g-factor and moment respectively, $q = eV_{zz}$. In an actual measurement, all the iron sites in a macroscopic and magnetically ordered sample are collectively measured. This is equivalent to taking the average of the last three factors in Equation 4.

Specifically, the spatial average of the angular factor $1/2\,(3\cos^2\theta - 1)$ yields zero. Therefore, in the magnetic ordered state of an amorphous magnetic solid there is nearly zero apparent quadrupole interaction, and the positions of the six spectral lines are symmetric with respect to the centroid. A closer inspection of the spectra of amorphous $Fe_{81.5}B_{14.5}Si_4$ (Fig. 1) indicates that although the positions of the six lines are symmetric about the centroid, the intensities of the six lines are not exactly symmetric. In particular, from the left, Peak 1 has slightly larger intensity than that of Peak 6. Similarly, in amorphous $Fe_{40}Ni_{40}B_{20}$ (Fig. 2) the intensity of Peak 2 is slightly larger than that of Peak 5. This may be due to the distribution of the isomer shift in the spectra of these samples. Such features were also observed by Chien *et al.* [5] for $Fe_{80}B_{20}$ amorphous alloy.

3.4. Spin-wave excitations

For all the amorphous ferromagnets investigated so far [11, 14, 15] the magnetic hyperfine field at low temperature is described by the well-known modified Bloch's law

$$\frac{\Delta H}{H(0)} = \frac{H(0) - H(T)}{H(0)} = B_{3/2}\left(\frac{T}{T_c}\right)^{3/2} + C_{5/2}\left(\frac{T}{T_c}\right)^{5/2} = BT^{3/2} + CT^{5/2} \quad (5)$$

where $B_{3/2}$ and $C_{5/2}$ are coefficients that can be related to fundamental quantities [16].

In non-crystalline ferromagnets the absence of a lattice makes it more difficult to understand the nature of spin waves. For long wavelengths, an effective medium approximation was proposed and agrees well with a quasi-crystalline approximation for spin-wave energy [17].

The leading $(T/T_c)^{3/2}$ term is characteristic of long-wavelength spin-wave excitations for which the non-periodic arrangement is not important [18]. This term was found to be dominant from 4.2 K up to temperatures as high as $T/T_c = 0.5$. In order to show the leading $T^{3/2}$ dependence, a plot of $-\log[\Delta H(T)/H(0)]$ against $\log T$ is given in Fig. 5 for the two alloys. The coefficients B and C are determined by fitting the data points with Equation 5 and are tabulated in Table III.

Fig. 6 shows plots of $[\Delta H(T)/H(0)][1/(T/T_c)]^{3/2}$ against T/T_c for the two samples; the intercept and the slope of the straight line give the values of $B_{3/2}$ and $C_{5/2}$. These values are summarized in Table III, in which one can see similar values for the two samples studied. For comparison, values of B, C, $B_{3/2}$ and $C_{5/2}$ for crystalline iron and nickel are also shown in Table III. The wide range of values of B and C for the glassy ferromagnets is in part due to the different values of the magnetic ordering temperature T_c. This behaviour indicates that the temperature dependence

TABLE III Coefficients B and C for glassy alloys $Fe_{81.5}B_{14.5}Si_4$ and $Fe_{40}Ni_{40}B_{20}$, and crystalline iron and nickel

Sample	$B(10^{-6}K^{-1})$	$C(10^{-8}K^{-1})$	$B_{3/2}$	$C_{5/2}$
$Fe_{81.5}B_{14.5}Si_4$	2.7 ± 0.2	1.312 ± 0.2	0.405 ± 0.05	0.117 ± 0.05
$Fe_{40}Ni_{40}B_{20}$	2.94 ± 0.2	0.615 ± 0.2	0.400 ± 0.05	0.11 ± 0.05
$Fe^{(4)}$	3.4 ± 0.2	0.1 ± 0.1	0.114 ± 0.007	0.04 ± 0.04
$Ni^{(4)}$	7.5 ± 0.2	1.5 ± 0.2	0.117 ± 0.003	0.15 ± 0.02

of the magnetization as $T \rightarrow 0$ could be described by Bloch's $T^{3/2}$ law.

The spin-wave excitations in glassy solids have been examined theoretically by using various models. The model discussed by Simposon [19] showed that structural disorder and variation in the exchange interaction leads to a larger $B_{3/2}$ coefficient. The introduction of disorder into crystalline ferromagnets leads to an increase in the spin-wave density of states for low energies of excitation [20]. The conclusion is consistent with the relatively larger $B_{3/2}$ values observed in amorphous ferromagnets.

As mentioned above, one of the peculiar results is that the leading $T^{3/2}$ term dominates over a very large temperature range. This effect, however, is related not only to the large values of B or $B_{3/2}$, but also to the values of C or $C_{5/2}$. As shown in Table III, for crystalline ferromagnets (e.g. nickel) $C_{5/2}/B_{3/2}$ is of the order unity, while it is of order 0.28 for the amorphous alloys studied. Following this argument, the results of smaller values of $C_{5/2}/B_{3/2}$ suggest that the mean exchange interaction does not extend much beyond the nearest neighbours.

3.5. Temperature dependence of $H(T)$

The magnetic ordering temperature T_c of amorphous $Fe_{81.5}B_{14.5}Si_4$ has been determined by reducing to zero the magnetic hyperfine interaction under no external magnetic field. This can be measured by the thermal scan method. The resultant spectrum is shown in Fig. 7. The number of counts is expected to show a rapid decrease at the magnetic ordering temperature, since the six-line magnetic spectrum then collapses to a paramagnetic doublet, centred about zero velocity with maximum absorption (see Fig. 1). The value of the magnetic ordering temperature as seen from Fig. 7 to be 608 ± 2 K. This value is in good agreement with those reported in the literature for similar amorphous alloys [14]. Fig. 7 shows also that the crystallization temperature T_{cr} for glassy $Fe_{81.5}B_{14.5}Si_4$ is about 650 K, i.e. about 40 K above T_c. Therefore, prolonged measurements at T close to T_c for a period did not induce crystallization in the sample. Also from Fig. 7 it is clear that the magnetic ordering temperature is sharply defined to within ± 8 K and there is no sign of a "smeared" transition. This result is similar to that for glassy $Fe_{40}Ni_{40}P_{14}B_6$ in which T_c = 537 K and is sharply defined to be within ± 2 K [14].

The relatively low value of the Curie temperature of the glassy ferromagnet $Fe_{81.5}B_{14.5}Si_4$ could be discussed as follows. By using the molecular-field result for the Curie temperature [5],

$$T_c = \frac{2Z_{av}J_{Fe\text{-}Fe}s(s+1)}{3k} \quad (6)$$

where s is the total spin, k is the Boltzmann constant and Z_{av} is the number of nearest neighbours. It has been argued that suitable changes in the atomic structure of amorphous Fe_xB_{100-x} ($72 \leqq x \leqq 88$) cause the value of T_c to decrease significantly with increasing iron content. As the iron concentration increases, the structure is supposed to change from a dense random packing structure to a body-centred cubic (b c c) type of structure so that Z_{av} in Equation 6 changes from about 12 to 8. It should be noted that the above scheme is based on the assumption that the average exchange interaction ($J_{Fe\text{-}Fe}$) remains constant, so that Z_{av} is reduced. However, X-ray diffraction measurements on amorphous-iron–metalloid alloys and amorphous iron suggest that there is no drastic change in the average coordination number [5]. Therefore, the large reduction of T_c ($x > 70$) is primarily the result of the decrease in the average exchange interaction J.

On the other hand, for temperatures close to T_c, the hyperfine field varies as a power law [14]:

$$H(T)/H(0) = D[1 - (T/T_c)]^{\beta} \quad (7)$$

where β and D are parameters which in the ideal case are β = 0.33 and D = 1.0.

Plots of log $[H(T)/H(0)]$ against log $[1 - (T/T_c)]$ for the ferromagnets $Fe_{81.5}B_{14.5}Si_4$ and $Fe_{40}Ni_{40}B_{20}$ are shown in Fig. 8. The critical parameters for the

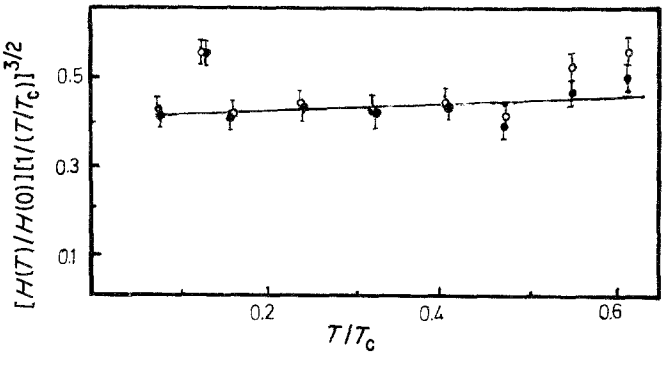

Figure 6 Changes of $[\Delta H/H(0)][(1/(T/T_c))]^{3/2}$ against reduced temperature for amorphous (○) $Fe_{81.5}B_{14.5}Si_4$, (●) $Fe_{40}Ni_{40}B_{20}$.

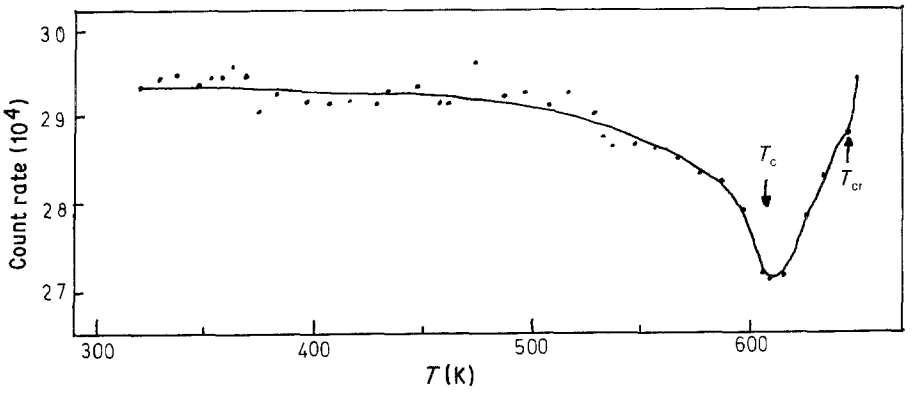

Figure 7 Count rate measured near the centroid of the spectrum as a function of temperature for amorphous $Fe_{81.5}B_{14.5}Si_4$.

ferromagnet $Fe_{81.5}B_{15.5}Si_4$ are $\beta = 0.323 \pm 0.03$ and $D = 1.0 \pm 0.05$. These values agree well with those obtained in similar amorphous ferromagnets [14].

The distribution of exchange interactions which are of particular importance in describing amorphous ferromagnets can be inferred from the temperature dependence of the MHF shown in Fig. 9, where the solid lines are a computer fit applying the statistical fluctuations in the exchange interaction constant (δ) and providing its variation as a function of temperature as shown in Fig. 10. It is clear that δ has a stability of ~ 0.5 over a temperature range $0.45 \leqq T/T_c \leqq 0.77$. It is known that the existence of metalloid atoms influence the magnetization through the mechanism of charge transfer. This implies, according to Fig. 10, that the effect of these atoms is to increase the degree of fluctuations at lower temperatures. A similar result was obtained for amorphous $Fe_{79}B_{16}Si_5$ [10].

To explain such results, the mean-field model [20] was considered. This model gives the fluctuations in the exchange interaction constant, J, as

$$\delta = (\langle \Delta J^2 \rangle / \langle J \rangle^2)^{1/2} \qquad 0 \leqq \delta \leqq 1 \qquad (8)$$

where $\delta = 0$ implies no variation in J. In ferromagnetic materials, J could be given by $J = 3KT_c/2Zs(s+1)$, where Z is the number of nearest neighbours and s is the spin. This formula shows that the fluctuations in $\Delta J/J$ should be strongly dependent on fluctuations in $\Delta Z/Z$. This behaviour could be due to structure modification in the direction of full crystallization, where it is known that $\delta = 0$ for crystalline ferromagnets.

3.6. Glassy-to-crystalline transition

As shown in Fig. 7, with further increase of temperature the count rate first increases slowly as a result of the second-order Doppler shift, and the decrease of the recoil-less fraction. The count rate suddenly increases at 645 ± 2 K. A rapid amorphous-to-crystalline transformation appears to have occurred, where after the crystallization temperature has been reached the amorphous state has been completely transformed into crystalline phases. Confirmation was obtained by taking Mössbauer measurements after cooling the sample down to room temperature. Fig. 11 shows the Mössbauer spectrum of the sample taken at room temperature, immediately after the second transition of Fig. 7 is completed. Analysis of Fig. 11 shows that the crystalline phases are α-Fe, Fe_2B and Fe–8 at % Si alloy, satisfying the condition of isomer shifts as shown in following Table IV.

4. Conclusions

The amorphous ferromagnets $Fe_{81.5}B_{14.5}Si_4$ and $Fe_{40}Ni_{40}B_{20}$ have been studied from 77.5 to 663 K by Mössbauer spectroscopy. The results show that the distribution in the magnetic hyperfine fields is due to the magnetic and isomer shift components only. The

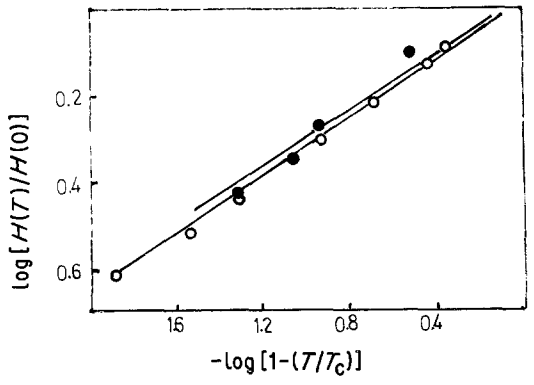

Figure 8 Change of $-\log [1 - (T/T_c)]$ against $-\log [H(T)/H(0)]$ for amorphous (○) $Fe_{81.5}B_{14.5}Si_4$, (●) $Fe_{40}Ni_{40}B_{20}$.

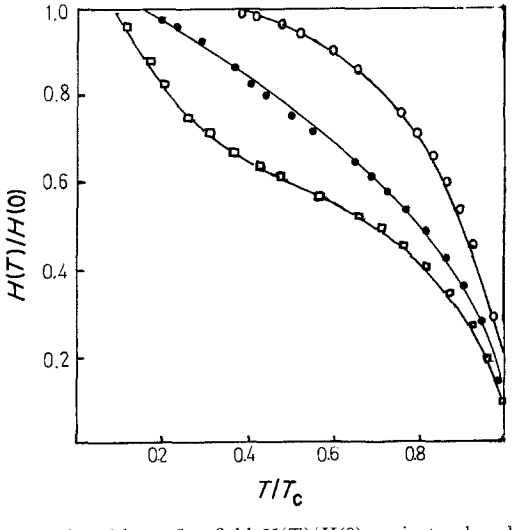

Figure 9 Reduced hyperfine field $H(T)/H(0)$ against reduced temperature for amorphous $Fe_{81.5}B_{14.5}Si_4$. δ = (○) 0, (●) 0.6, (□) 0.8.

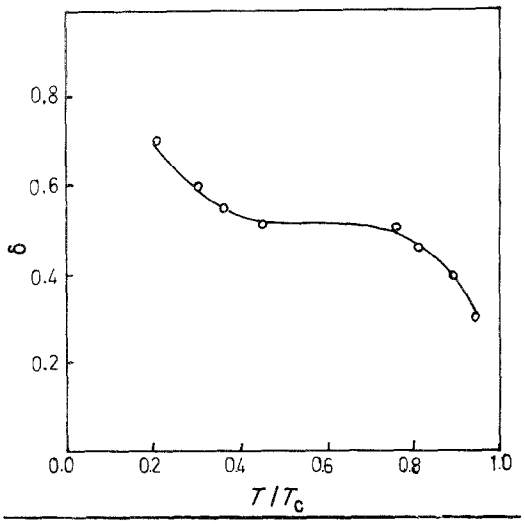

Figure 10 The fluctuation in the exchange interaction constant (δ) as a function of reduced temperature T/T_c.

$T^{3/2}$ and $T^{5/2}$ behaviours of the glassy ferromagnets were recognized by the change of MHF as a function of $(T/T_c)^{3/2}$. At low temperature, $H(T)/H(0)$ has a temperature dependence $[1 - B_{3/2}(T/T_c)^{3/2} \ldots]$ in a large temperature range due to long wavelength spin-wave excitations. The value of the coefficient $B_{3/2} = 0.40$ is almost four times larger than those of crystalline iron and nickel. The reduced hyperfine field $H(T)/H(0)$ rapidly decreases with the reduced temperature T/T_c as a result of the distribution of exchange interactions. Theoretical calculations using the molecular-field approximation with the inclusion of a distribution of exchange interactions can only qualitatively describe the observed results.

The magnetic ordering temperature $T_c = 608$ K for amorphous $Fe_{81.5}B_{14.5}Si_4$ is found to be sharply defined within ± 2 K. At temperatures below T_c, the reduced hyperfine field varies as $D(1 - T/T_c)^{\beta}$ with $D = 1.00 \pm 0.05$ and $\beta = 0.3 \pm 0.03$.

TABLE IV Room-temperature Mössbauer parameters for $Fe_{81.5}B_{14.5}Si_4$

Phase	I.S. (mm sec^{-1})	MHF (T)	Relative area
α-Fe	Zero	33	0.026
Fe_2B	0.13	23.2	0.35
Fe–8% Si	0.1	31.2	0.62

At $T > 593$ K the glassy state is paramagnetic, and a well-defined quadrupole spectrum consisting of two peaks is observed. However, the observed asymmetrical doublets suggest that the electronic states of iron in the samples are not identical. The quadrupole splitting is essentially temperature-independent.

A fully crystalline material from amorphous $Fe_{81.5}B_{14.5}Si_4$ was obtained at 645 ± 2 K and contained three different crystalline phases, namely α-Fe, Fe_2B and Fe–8% Si.

References

1. Proceedings of the Conference on Metallic Glasses: Science and Technology, edited by D. Hargitai, I. Bakonyi, and T. Kemeny, Hungary, 1981 (Kultura, Budapest, 1981).
2. Proceedings of Rapidly Quenched Metals IV (The Japan Institute of Metals, Sendai, 1982).
3. A. I. GUBNOV, *Fiz. Tverd. Tela (Leningrad)* **2** (1960) 502.
4. C. L. CHIEN, *Phys. Rev. B* **18** (1978) 1003.
5. C. L. CHIEN, D. MUSSER, E. M. GYORGY, R. C. SHERWOOD, H. S. CHEN, F. E. LUBORSKY and J. L. WALTER, *ibid.* **20** (1979) 283.
6. N. BANERJEE, R. ROY, A. K. MAJUMDAR and R. HASEGAWA, *ibid.* **24** (1981) 6801.
7. H. N. OK and A. H. MORRISH, *ibid.* **22** (1980) 4215.
8. N. SAEGUSER and A. H. MORRISH, *ibid.* **26** (1982) 10.
9. P. J. SCHURER and A. H. MORRISH, *ibid.* **20** (1979) 4660.
10. A. A. BAHGAT and E. E. SHAISHA, *J. Non-Cryst. Solids* **56** (1983) 243.
11. A. A. BAHGAT, *Phys. Status Solidi (a)* **63** (1981) K39.
12. A. A. BAHGAT, *ibid.* **63** (1981) K39.

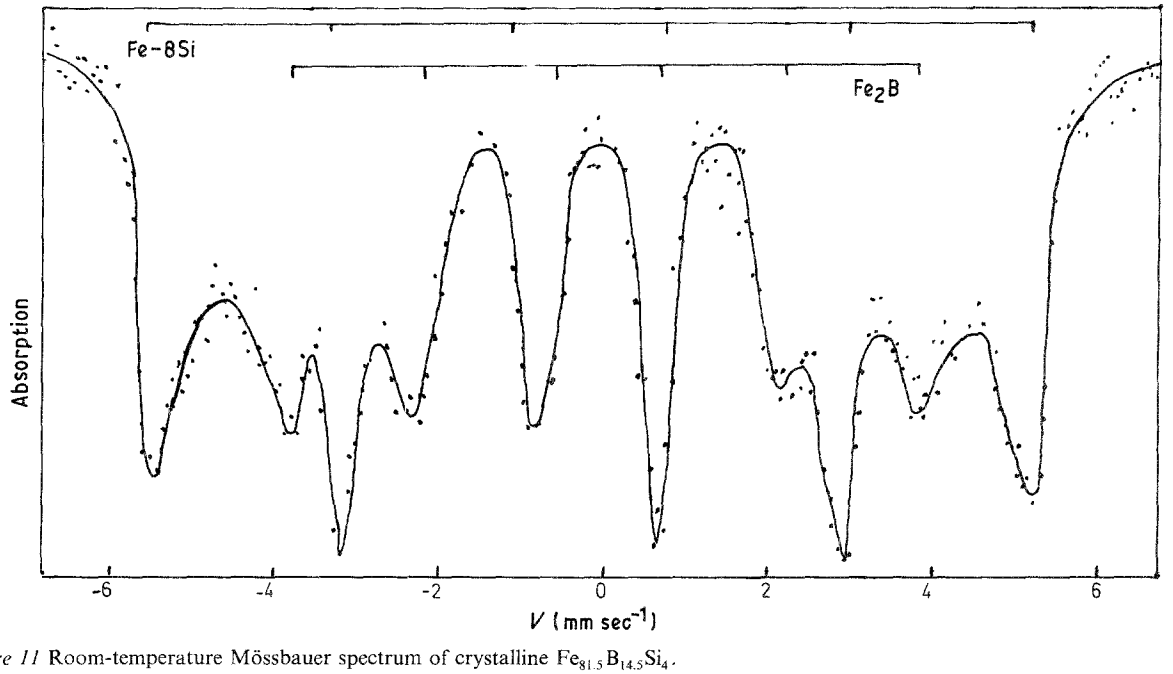

Figure 11 Room-temperature Mössbauer spectrum of crystalline $Fe_{81.5}B_{14.5}Si_4$.

13. R. W. COCHRANE and J. O. STROM-OSLEN, *J. Phys. F* **7** (1977) 1799.
14. C. L. CHIEN and R. HASEGAWA, *Phys. Rev. B* **16** (1977) 3024.
15. *Idem, ibid.* **16** (1977) 2115.
16. W. MARSHALL and S. W. LOVESEY, "Theory of thermal neutron scattering" (Oxford University Press, London, 1971).
17. V. A. SINGH and L. M. REITH, *J. Appl. Phys.* **49** (1979) 1642.
18. C. HERRING and C. KITTEL, *Phys. Rev.* **81** (1951) 869.
19. A. W. SIMPOSON, *Wiss. Z. Tech. Univ. Dresden* **3** (1974) 1020.
20. T. KANEYOSHI and R. HOMURA, *J. Phys. C* **5** (1972) L65.

Received 21 April
and accepted 11 November 1986